LYMPHOID NEOPLASIA

Human mesenchymal stromal cells deliver systemic oncolytic measles virus to treat acute lymphoblastic leukemia in the presence of humoral immunity

Anna Castleton,[1] Aditi Dey,[1] Brendan Beaton,[1] Bella Patel,[1] Anne Aucher,[2] Daniel M. Davis,[2,3] and Adele K. Fielding[1]

[1]Department of Hematology, University College London, London, United Kingdom; [2]Department of Life Sciences, Imperial College London, London, United Kingdom; and [3]Manchester Collaborative Center for Inflammation Research, University of Manchester, Manchester, United Kingdom

Key Points

- Human BM-MSCs can be used to successfully deliver systemic oncolytic measles virotherapy to ALL tumor targets.
- This approach permits circumvention of preexisting anti-measles humoral immunity and enhanced therapeutic outcomes.

Clinical trials of oncolytic attenuated measles virus (MV) are ongoing, but successful systemic delivery in immune individuals remains a major challenge. We demonstrated high-titer anti-MV antibody in 16 adults with acute lymphoblastic leukemia (ALL) following treatments including numerous immunosuppressive drugs. To resolve this challenge, human bone marrow–derived mesenchymal stromal cells (BM-MSCs) were used to efficiently deliver MV in a systemic xenograft model of precursor B-lineage–ALL. BM-MSCs were successfully loaded with MV ex vivo, and MV was amplified intracellularly, without toxicity. Live cell confocal imaging demonstrated a viral hand-off between BM-MSCs and ALL targets in the presence of antibody. In a murine model of disseminated ALL, successful MV treatment (judged by bioluminescence quantification and survival) was completely abrogated by passive immunization with high-titer human anti-MV antibody. Importantly, no such abrogation was seen in immunized mice receiving MV delivered by BM-MSCs. These data support the use of BM-MSCs as cellular carriers for MV in patients with ALL. (*Blood*. 2014;123(9):1327-1335)

Introduction

Adult acute lymphoblastic leukemia (ALL) is an aggressive hematological malignancy with complete remission rates following initial induction therapy of 85% to 95%.[1-8] Despite cycles of combined immunosuppressive and myelosuppressive chemotherapeutics, long-term survival is achieved in fewer than half of adults,[9] and few patients with relapsed disease survive.[10] The ability to quantify and monitor minimal residual disease in the majority of patients with ALL, provides a basis—already recognized by the regulatory authorities—for early intervention with novel therapeutics prior to overt disease relapse,[11] which would be the optimal setting for novel biological therapies.

Oncolytic viruses (OVs) preferentially infect and lyse transformed cells, leaving normal cells relatively unharmed. They lack cross-resistance with existing therapies, and the acceptable safety profile of OVs has been demonstrated in numerous trials.[12-16] Vaccine-strain live, attenuated MV (MV-Edm) has shown tumor-specific replication and antitumor activity in a range of malignancies,[17-30] with published phase 1 clinical trials showing safety and some therapeutic promise in cutaneous T-cell lymphoma[31] and ovarian cancer.[32] Sophisticated manipulations of the vaccine MV genome can aid tumor targeting[33-37] and assist with in vivo tracking.[21,38,39] Despite this, the necessity to shield MV from neutralizing antibody during systemic delivery has not been appropriately addressed[40,41] but is likely to preclude repeat dosing regimes and impact adversely on therapy.

There has been increasing interest in cell-based delivery systems to circumvent humoral immunity. Success of this strategy depends on efficient ex vivo cellular loading with virus, intracellular virus amplification, effective cellular targeting of tumor sites following systemic administration, and successful virus hand-off at the tumor site. A variety of primary leukocytes,[42-44] immortalized cell lines,[45] and progenitor cells[41,46-48] have all undergone preclinical evaluation for this purpose, with varying degrees of therapeutic success. In reality, many of the potential candidates are technically difficult to isolate, culture, or expand ex vivo. Mesenchymal stromal cells (MSCs) are nonhematopoietic cells with the capacity to self-renew and differentiate into cell lineages of mesenchymal origin. They can be isolated from a number of different sources. In the present study, we used a murine model of disseminated ALL to investigate the ability of primary human bone marrow–derived MSCs (BM-MSCs) to act as cellular carriers, effectively delivering systemic measles virotherapy to mice passively immunized with high levels of human anti-MV antibodies.

Methods

Primary cells and cell lines

BM samples were obtained from consenting healthy volunteers undergoing BM harvest. Mononuclear cells, isolated by density gradient centrifugation

Submitted September 24, 2013; accepted November 27, 2013. Prepublished online as *Blood* First Edition paper, December 17, 2013; DOI 10.1182/blood-2013-09-528851.

The online version of this article contains a data supplement.

There is an Inside *Blood* commentary on this article in this issue.

The publication costs of this article were defrayed in part by page charge payment. Therefore, and solely to indicate this fact, this article is hereby marked "advertisement" in accordance with 18 USC section 1734.

(Ficoll, Amersham Biosciences, Bucks, United Kingdom [UK]) were resuspended in MesenCult MSC media plus MesenCult stimulatory supplements (StemCell Technologies, Grenoble, France) and 1 ng/mL basic fibroblast growth factor (R&D Systems, Minneapolis, MN). Cells were plated at 1×10^7/25 mL, and nonadherent cells were removed after 1 to 2 days. Vero cells (CCL-81; ATCC) were maintained in Dulbecco's modified Eagle medium (Gibco/Invitrogen, Paisley, UK) supplemented with 5% heat-inactivated fetal bovine serum (Gibco/Invitrogen). Nalm-6 cells (ACC-128; DSMZ) were maintained in RPMI 1640 medium (Gibco/Invitrogen) supplemented with 10% fetal bovine serum. For in vivo precursor B-cell (B)-ALL xenograft models, we generated stably transduced Nalm-6-luc, using MoMLV vector encoding firefly luciferase (gift from Dr Martin Pule, United College London) and pCL-ampho packaging vector (Imgenex).

BM-MSC characterization

International Society for Cellular Therapy[49] criteria were used to characterize BM-MSCs. Cells were assessed at passages 1 to 3 to confirm successful isolation and purity. Passages 3 to 7 BM-MSCs were used for experiments.

Measles virus production and cellular infection

Live, attenuated MV-NSe– or green fluorescent protein (GFP)-expressing counterpart was used for all experiments. MV was propagated on Vero cells at a multiplicity of infection (MOI) of 0.01 using standard techniques and titrated on Vero cells using the modified Kärber formula.[50] For infection of BM-MSCs, cells were washed with phosphate-buffered saline (PBS), inoculated with virus in OptiMEM at the appropriate MOI, and incubated for 2 hours at 37°C before removing the virus and replacing with fresh medium. The time point after infection is taken from completion of the inoculation period. Fusion inhibitory peptide (FIP; Z-D-Phe-Phe-Gly-OH; Bachem; Switzerland) was added at 40 μg/mL.

MV nucleocapsid mRNA quantification by real-time quantitative-polymerase chain reaction

MV nucleocapsid (MV-N) mRNA was quantified by customized TaqMan gene expression real-time polymerase chain reaction (PCR) assay (Applied Biosystems). cDNA was mixed with 0.9 mM forward and reverse primers and a 0.25 mM TaqMan probe and labeled with FAM reporter dye. Triplicate reactions were run on an ABI 7500 (Applied Biosystems) with nontemplate controls in each plate. PCR cycle number at threshold is represented as Ct. Relative expression level of gene of interest was calculated using the $2^{(-\Delta\Delta Ct)}$ formula.[51]

MV-H glycoprotein immunostaining

Cells were fixed at room temperature in 10% formalin, washed and incubated with anti-H antibody (Chemicon; 1:100 final dilution) or mouse IgG1 K (MOPC21; 1 μg/mL; Sigma-Aldrich), followed by polyclonal goat anti-mouse Biotin IgG (Sigma-Aldrich; 1:400), horseradish peroxidase streptavidin (Dako; 1:500), 3-amino-9-ethylcarbazole+ High Sensitivity Substrate Chromogen (Dako), and counterstained using Carrazi's hematoxylin.

Viability assays

For the 3-(4,5 dimethylthiazol-2-yl)-5-(3-carboxymethoxyphenyl-2-(4-sulfophenyl)-2H-tetrazolium (MTS) assay, BM-MSCs were plated in triplicate at 5×10^4 cells/mL in round-bottomed 96-well plates and infected with MV-NSe for 24 hours. At appropriate time points, 20 μL of MTS reagent (CellTiter-96 AQeous MTS powder, reconstituted at 2 mg/mL; Promega) was added and read after incubation for 4 hours at 37°C (target absorption peak, 490 nm; reference, 650 nm) on a Tecan Sunrise absorbance reader (Jencons-PLS). Trypan blue viability dye was used to enumerate viable cells.

Xenograft models

CB17 severe combined immunodeficient (SCID) mice (Charles River Laboratories, Margate, UK) were housed in accordance with UK home office–approved protocol and used at 6 to 8 weeks old. For assessment of MV-infected BM-MSC localization to established ALL xenografts, 1×10^6 viable Nalm-6 cells (in 200 μL PBS) were injected intravenously (IV). After 3 weeks, intra-BM (IBM) sampling was performed to confirm leukemia engraftment (supplemental Methods on the *Blood* Web site). Ten days later, animals received 1×10^6 MV-luc–loaded BM-MSCs (or PBS control) IV. The fate of infected BM-MSCs was determined by bioluminescent imaging. Shaved animals were given 200 μL D-Luciferin (Caliper Life Sciences, Cheshire, UK) intraperitoneally (IP) and imaged under anesthetic using an IVIS 100 Lumina (Caliper Life Sciences, Cheshire, UK). Analysis was with Living Image 3.2 software. To assess therapeutic efficacy, disseminated ALL xenografts were established by IV injection of 1×10^6 viable Nalm-6-luc cells (in 200 μL PBS). Weekly bioluminescent imaging was performed from week 3 onward. As treatment, 6 consecutive weekly IV injections of 1×10^6 pfu MV-NSe, 1×10^6 BM-MSCs preloaded with MV-NSe at an MOI of 1.0, or 1×10^6 BM-MSCs alone were given, starting 3 days after tumor administration. Passively immunized mice received 50 IU anti-MV IgG IP, 3 hours before each MV injection. The primary end point was survival to humane end point, with the secondary end point being disease burden (assessed by bioluminescence imaging or by flow cytometric quantification).

Live cell imaging

BM-MSCs (5×10^3) were infected with MV-NSe-GFP (MOI of 1) for 2 hours and cultured in 8-well chambered coverglasses (Chambered Borosilicate Coverglass; Laboratory-Tek). After 48 hours, 75×10^3 Nalm-6 cells expressing red fluorescent protein (RFP) were added and directly imaged by resonance laser scanning confocal microscopy (TCS SP5 RS; Leica) using excitation wavelengths of 488 and 594 nm with 20× dry and 63× water immersion objectives (not applicable = 1.2) and analyzed by Volocity (National Institutes of Health).

Enzyme-linked immunosorbent assay

Measles virus IgG antibody was quantified in duplicate using a solid phase enzyme-linked immunoassay (IBL International; RE57141). Optical density (OD) was measured at 450 nm (reference wavelength, 650 nm) using a Tecan Sunrise absorbance reader (Jencons-PLS). The concentration of samples was determined directly from the standard curve. Titers of 200 mIU/mL or higher were deemed MV immune.

Statistical analysis

Graphs were plotted using Prism 5.0 (GraphPad Software) and Microsoft Excel. Data are presented as mean, with error bars shown as standard error of the mean) where appropriate. Statistical analysis of survival curves was performed using the log-rank test. For all other analyses, unpaired Student *t* test or Mann-Whitney U test was used. $P \leq .05$ was considered statistically significant.

Results

Anti-MV antibody titers remain high in adult ALL patients despite several months of intensive immunosuppressive therapy

The effect of immunosuppressive combination chemotherapy as delivered to adults with ALL on MV antibody titers is not known. We quantified anti-measles IgG antibody titers using an enzyme immunoassay in sera from 16 patients treated on the UK multicenter ALL trial UKALL14 (NCT01085617) both prior to and after up to 3 months of continuous therapy. Diagnostic sera were paired with samples taken at 1 of 2 time points following completion of a minimum of 8 weeks of chemotherapy including high-dose dexamethasone, vincristine, daunorubicin, L-asparaginase, rituximab, 6-mercaptopurine, cytarabine, and cyclophosphamide. Surprisingly, anti-MV IgG antibody

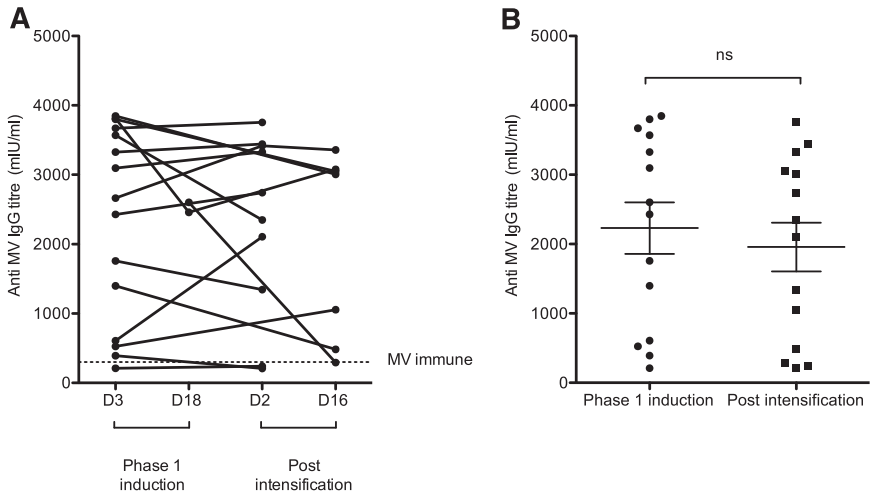

Figure 1. Intensive immunosuppressive therapy for ALL does not suppress anti MV IgG production in patients on the UKALL14 trial. (A) Graph showing anti-MV IgG titer (y-axis) as quantified by enzyme-linked immunosorbent assay. Paired sera from 16 patients participating in the UKALL14 trial were evaluated at a minimum of 2 time points (x-axis). Each dot represents a value, with a line connecting each patient's individual values. The dotted line represents the level at which a human is considered immune to measles virus infection. (B) Graph showing individual values with mean (horizontal line) and standard error of the mean (SEM; error bars) of anti-MV IgG (y-axis) for the 12 patients with samples from the earliest (day 3 of therapy) and latest time points (after 3 months of intensive inpatient therapy). There is no significant difference between the 2 time points.

titers persisted at clinically significant levels despite this intensive chemotherapy regimen (Figure 1A-B).

BM-MSCs can be infected by oncolytic measles virus ex vivo and serve as effective virus producing units

MSCs were prepared from normal human BM, and their appropriate characteristics were demonstrated (supplemental Figure 1). To confirm the susceptibility of BM-MSCs to MV infection ex vivo, we evaluated cell surface expression of the known MV receptors CD46, CD150, and nectin 4 by flow cytometry. BM-MSCs consistently expressed vaccine strain receptor CD46, whereas the wild-type receptor CD150 and the epithelial receptor nectin 4 were not expressed (supplemental Figure 2). We then determined the optimum MOI and time point postinfection, at which maximal virus productivity occurs with minimum BM-MSC death. We infected BM-MSCs with MV-GFP at various MOIs and compared GFP expression daily postinfection. GFP positivity consistently showed a peak in intensity at 48 hours postinfection (hpi). Photomicrographs of representative experiments at 48 hpi with an MOI of 1.0 are shown in Figure 2Ai, demonstrating MV cytopathy, with widespread GFP-positive multinucleate syncytia. Cell surface MV-H glycoprotein expression correlated closely with GFP expression, reaching maximal intensity at 48 hpi (Figure 2Aii). The viability of BM-MSCs was formally assessed by MTS assay. Figure 2B shows relative cell proliferation at each time point for each MOI. At an MOI of 1.0, there was no significant difference in cell viability between time points. Subsequently, we determined viral genome by real-time quantitative-PCR quantification of MV-N mRNA (Figure 2Ci-ii) and cell-associated and supernatant virus output by $TCID_{50}$ (Figure 2Di-iii). No increment in MV-N mRNA was seen above an MOI of 1.0, and $TCID_{50}$ data confirmed a peak in cell-associated virus productivity at 48 hpi. Notably, there was almost no virus shed into the supernatant. Finally, we demonstrated that on reducing virus-mediated cell-cell fusion and multinucleate syncytia formation by the postinfection addition of FIP to cell culture medium, cell-associated virus titers were higher at all time points postinfection (Figure 2Ei-iii), with a trend toward statistical significance at later time points. Trypan blue viability assay confirmed a reduction in MV-specific cell death for cells cultured with FIP compared with those cultured without (data not shown). Taken together, the data shown in Figure 2 confirm optimal conditions for ex vivo BM-MSC loading, using an MOI of 1.0 at a standard inoculation time of 2 hours and postinoculation culture in the presence of FIP. Harvest of loaded BM-MSCs was performed at 24 hpi to allow delivery at the optimal 48-hour productivity time point.

MV-loaded BM-MSCs localize to sites of ALL in the BM following intravenous infusion

To evaluate the ability of ex vivo loaded BM-MSCs to localize to established sites of ALL, we used a previously characterized model of disseminated precursor B-ALL.[22] Six- to 8-week-old SCID mice were injected with 1×10^6 Nalm-6 cells IV. After 3 weeks, IBM sampling from the right femur confirmed tumor cell engraftment in all mice as demonstrated in representative flow cytometry plots (Figure 3A). Ten days later, to minimize the potentially confounding issue of BM-MSC homing toward injured tissues, passage 3 BM-MSCs were loaded ex vivo with MV-luc at an MOI of 1.0 and at 24 hpi, injected IV at 1×10^6 cells per mouse, with control mice receiving PBS alone. The fate of infected cells was tracked using daily bioluminescent imaging for 10 days. Representative images in Figure 3B confirm early localization of MV-infected BM-MSCs to lung parenchyma, consistent with first pass entrapment. Subsequently, the bioluminescence signal relocalized to the ALL-containing BM, confirming the ability of MV-luc to reach distant tumor targets when delivered IV within BM-MSC. Furthermore, in 2 of 3 animals, bioluminescence colocalized to the opposite side to that used for IBM sampling, proving that homing is not solely related to injury from sampling method.

BM-MSCs allow successful virus delivery to tumor targets in the presence of humoral immunity

Next, we assessed the ability of BM-MSCs to deliver MV to ALL cells in the presence of preexisting neutralizing antibodies. Human anti-MV antisera were obtained from discard specimens. Anti-MV IgG was titrated in pooled, heat-inactivated sera using an enzyme immunoassay. MV-loaded BM-MSCs or naked MV was treated with serial dilutions of high titer anti-MV antibody serum ex vivo, before being overlaid onto the standard MV culture cell line, Vero. MV hand-off from BM-MSC to Vero was quantified by syncytia formation at 48 hours after overlay (Figure 4A). Naked MV was very effectively neutralized by anti-MV IgG—with syncytia being evident only at very low concentrations of antibody—1:256 or higher dilution. When Vero cells were overlaid with MV-infected BM-MSCs, significantly more syncytia were seen at all antibody concentrations. MV-infected BM-MSCs permitted MV hand-off, at high antibody concentrations (1:8 dilution), a 5-fold higher concentration

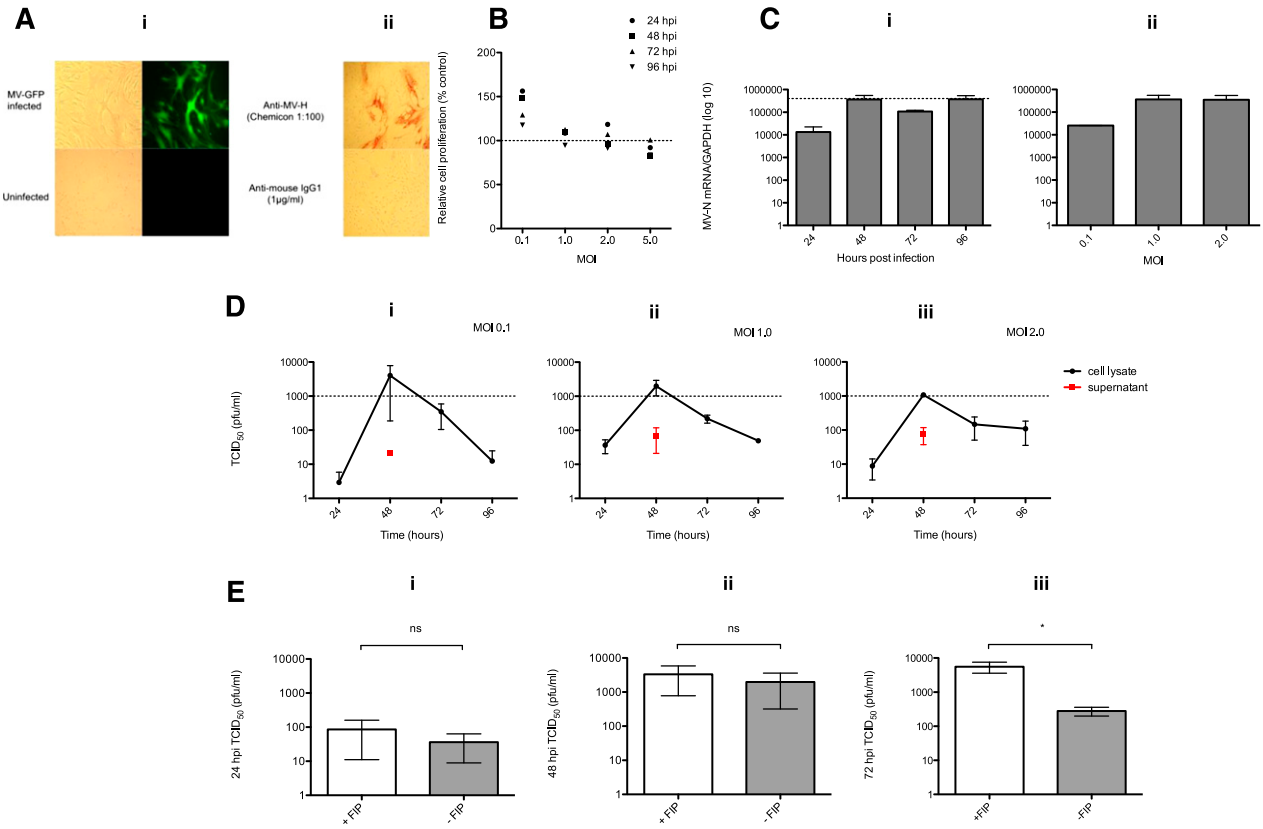

Figure 2. BM-MSCs support MV infection ex vivo and act as viable virus producing units. BM-MSCs were infected with MV-NSe-GFP at a range of MOIs, and assessed at 24-hour time points. (A) Representative images taken (Nikon Eclipse; TS100; ×20 objective) at 48 hours postinfection (hpi) at MOI 1.0 demonstrating (i) GFP positivity within multinucleate syncytia (uninfected cells as control) and (ii) cell surface MV-H glycoprotein expression (infected, isotype stained cells shown as negative control. Additional negative control was performed on uninfected cells (data not shown). (B) MTS colorimetric assay performed on infected BM-MSCs at 24-hour time points after infection for a range of MOIs. Mean values from 2 independent experiments carried out in at least triplicate are shown as a percentage of the mean values from uninfected controls. (C) Graph shows measles virus nucleocapsid (MV-N) RNA production by infected BM-MSCs at 24-hour time points postinfection with MOI of 1.0 (i) and at 48 hours postinfection for a range of MOIs (ii). Mean ± SEM. N = 3. (D) Graphs show $TCID_{50}$ data for MV-infected BM-MSCs at 24-hour time points postinfection with MOIs of (i) 0.1, (ii) 1.0, and (iii) 2.0, performed on cell lysates and supernatants. For supernatants, all time points postinfection were tested, with virus only detectable at 48 hpi for all conditions. Mean ± SEM. N = 3 to 5. (E) Graphs show $TCID_{50}$ data for BM-MSCs infected with MOI of 1.0 and cultured in the presence or absence of FIP. Data are for (i) 24 hpi (P = .4), (ii) 48 hpi (P = .25), and (iii) 72 hpi (*P = .05) and are shown as mean ± SEM. N = 3 to 5.

than the minimum concentration (1:256 dilution) permissive to infection when naked MV is used. These data confirm the ability of BM-MSCs to protect MV against antibody neutralization in vitro. Using a dual color system, we performed live cell confocal microscopy to directly visualize virus hand-off between Nalm-6 ALL cells, stably transduced to express RFP and green MV-GFP–infected BM-MSCs. Representative images shown in Figure 4B demonstrate the different stages of a fusion event between a single red Nalm-6 cell and a large MV-GFP–infected BM-MSC syncytium, taking place over 20 minutes of coculture (representative live cell imaging in supplemental Video 1). The Nalm-6 cell is seen to transition from red, becoming yellow as heterofusion takes place, and subsequently green as MV-GFP hand-off occurs. Corresponding brightfield images are shown beneath each fluorescent image. We used the live cell imaging to probe the role of anti-MV antibodies in the BM-MSC-to-ALL cell fusion/hand-off process. As indicated in Figure 4C, cells were preincubated with anti-MV antibody containing serum diluted either 1:4 (positive control, expected from data in Figure 4A to block fusion in both conditions) or 1:128 (the highest antibody concentration expected to discriminate between the 2 conditions), or with FIP as an additional positive control. Figure 4Ci-ii shows the percentage of Nalm-6 cells fusing with infected BM-MSCs or the ratio of RFP:GFP following 80 minutes of coculture. When anti-MV antibodies are absent, up to 40% of cells in contact demonstrated heterofusion within this time frame. Although fusion was predictably and significantly ablated in the presence of 1:4 serum dilution, or with FIP (positive control), no significant difference in heterofusion was observed in the presence of 1:128 serum dilution, with just >20% of cell-cell heterofusion events remaining, ie, half the level of the negative control condition. To be certain that anti-MV antibody did not affect contact time between cells rather than prevent fusion, BM-MSC-to-ALL cell contact time in the presence of 1:128 serum dilution was quantified for at least n = 125 events. The majority of heterofusion events were rapid, occurring within 20 minutes of coculture (Figure 4D) indicating that contact time between ALL and BM-MSC did not significantly change with the addition of anti-MV antibody. Taken together, the data in Figure 4 illustrate the ability of MV-infected BM-MSCs to readily hand off viable replicating MV to noninfected ALL cell targets, with BM-MSCs affording MV significant protection against neutralizing antibodies in vitro. A proportion of the virus hand-off occurs via the rapid process of carrier cell-to-tumor cell heterofusion.

BM-MSCs enhance the therapeutic efficacy of systemically delivered measles virotherapy in the presence of preexisting high titer anti-MV antibodies

We then determined whether the in vitro findings could be translated into therapeutic efficacy in an SCID murine model of precursor

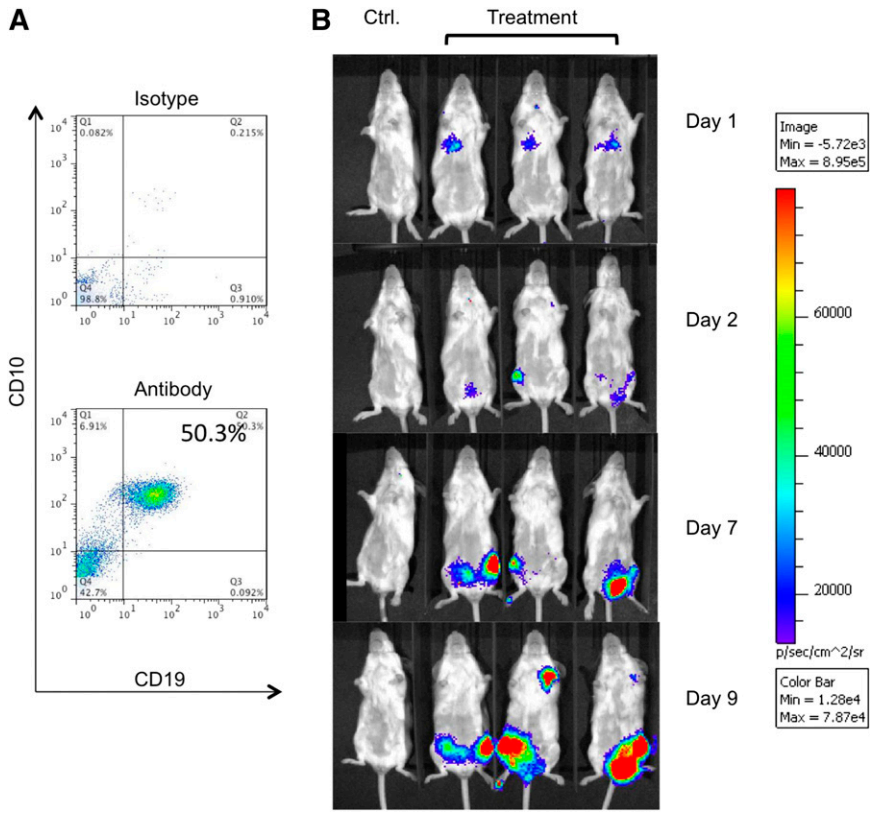

Figure 3. Systemically administered MV-infected BM-MSCs show early passive lung entrapment and subsequent relocalization to leukemic bone marrow. SCID mice with established Nalm 6 xenografts received intravenous injection with BM-MSCs infected with MV-luc. (A) Representative flow cytometry plots of murine bone marrow performed prior to administration of infected carrier cells, confirming the presence of CD19 (x-axis) and CD10 (y-axis) expressing leukemic populations. Gating was of live cells based on forward scatter and side scatter characteristics, with appropriate isotypes used as negative controls. (B) Representative bioluminescence images of SCID mice following systemic injection with MV-luc–infected BM-MSCs. Mice receiving PBS only were used as controls to account for background luminescence. For treatment group, N = 3.

B-ALL. Six- to 8-week-old SCID mice received IV injection with 1×10^6 Nalm-6 cells stably transduced to express firefly luciferase. On day 2, mice received IV injections of 1×10^6 plaque forming units (pfu) MV-NSe, 1×10^6 BM-MSCs loaded ex vivo (24 hours prior) with MV-NSe at an MOI of 1.0, or 1×10^6 uninfected BM-MSCs. Treatments continued weekly for a total of 6 weeks. Groups were further divided into mice receiving passive immunization with 50 IU anti-measles IgG, delivered IP 3 hours before each therapy injection or those receiving PBS as a control. Tumor burden was quantified by bioluminescent imaging. OS was plotted using the method of Kaplan-Meier. Figure 5A shows the OS of all mice by treatment allocation. As expected, mice receiving only MSCs rapidly succumbed to ALL (median survival, 53 days), with significantly inferior outcome compared with either MV alone or MV-MSC alone ($P \leq .0001$ and $P = .0027$, respectively), clearly confirming the lack of therapeutic benefit of MSCs in this model. Naked MV enhanced survival, as expected. This effect is abrogated in the presence of anti-MV antibody (median survival, 64 days), with comparison of survival curves for naked MV treatment group vs naked MV [+ab] showing a statistically significant difference ($P = .0013$). Mice receiving MSC-delivered MV had the best antitumor responses (median survival > 100 days) with all animals surviving to the end of the experiment and significantly superior responses compared with standard naked MV treatment groups (MV [+ab] vs MV-MSC [+ab], $P = .0022$; MV alone vs MV-MSC alone, $P = .0234$). The administration of anti-MV antibody to mice receiving MV within MSCs did not abrogate the therapeutic effect at all. (Survival curve comparisons are reiterated in supplemental Table 1.) Figure 5B shows representative bioluminescent imaging performed at equivalent time points, pictorially representing the relative tumor burdens for animals in the different treatment groups. Figure 5C shows the week 6 tumor burden measurements, as assessed by bioluminescent activity for each animal, minus the background luminescence. The data in Figure 5A,C confirm a statistically significant therapeutic benefit of delivering MV within BM-MSCs in the presence of anti-MV humoral immunity. To ensure that any technical problems with ALL engraftment had not biased the results, flow cytometric evidence of ALL was sought at experiment termination in the BM of every animal in which bioluminescence did not show overt disease. All mice had some flow cytometric evidence of leukemia within the BM at termination (data not shown). These data confirm our previous finding that systemically administered MV can successfully treat mice with aggressive disseminated ALL. We showed that anti-MV antibody abrogates this therapeutic potential. However, administration of MV inside BM-MSC carriers protects the virus against antibody neutralization, allowing an ongoing therapeutic effect of systemically administered virus against disseminated tumor in the presence of high titer antibody.

Discussion

We have previously shown that disseminated precursor B-ALL xenografts in SCID mice are highly sensitive to MV-mediated oncolysis.[22] For our planned phase 1 trial in patients with relapsed ALL, the coadministration of various immunosuppressive anti-ALL agents such as cyclophosphamide, steroid, or anti-B-cell monoclonal antibodies alongside MV therapy is under consideration, with the aim of suppressing an anti-MV response. This rationale is based on murine data suggesting that clinically approved cyclophosphamide regimens can suppress humoral anti-MV and anti-vesicular stomatitis virus responses.[52] However, our data show, on sera samples taken from a subset of UKALL14 trial participants before and after intensive

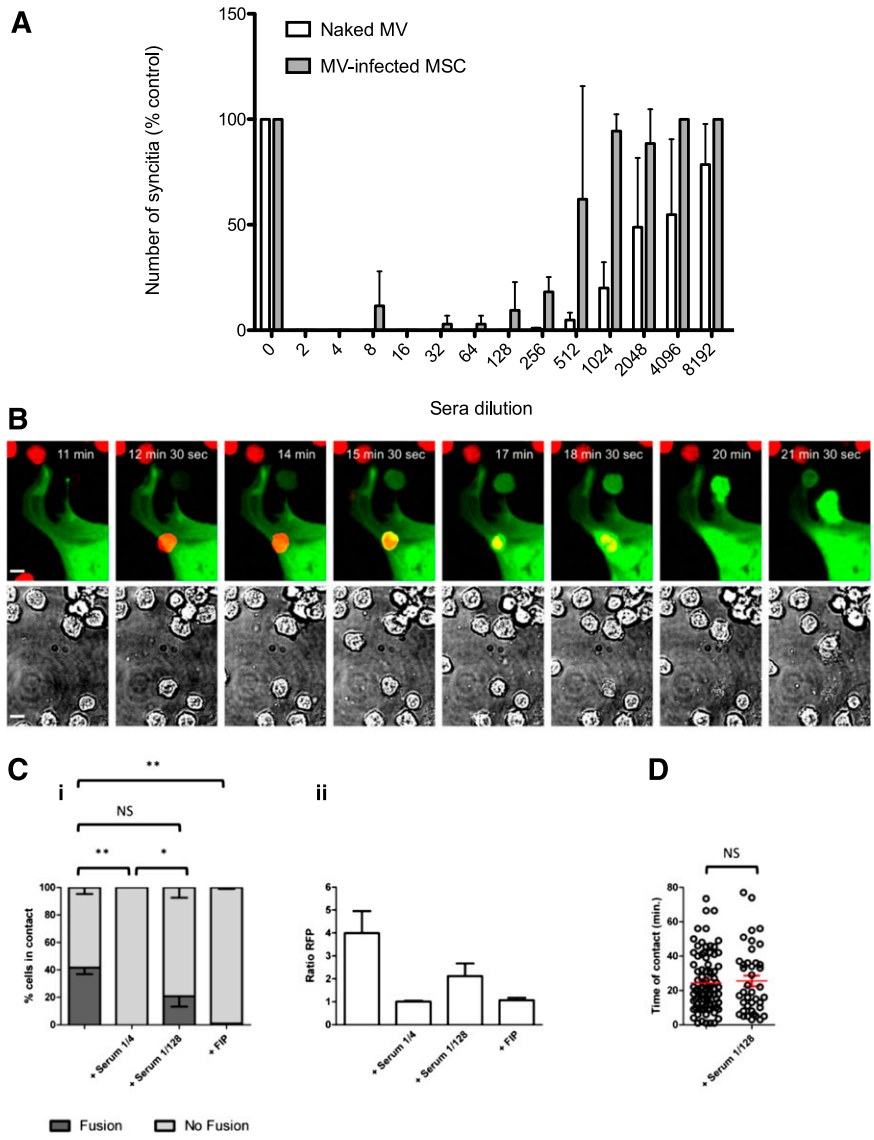

Figure 4. MV infected BM-MSCs permit fusion and virus hand-off to target cells in the presence of anti-MV antibody. (A) Graphs show Vero cell syncytia quantification at 48 hours postoverlay with MV-NSe–loaded BM-MSCs or naked MV-NSe pretreated with dilutions of high titer anti-MV antibody. Total numbers of syncitia from each well of a 96-well plate were counted. Data are represented as a percentage of virus control (MV-infected cells with no serum pretreatment; x-axis) in relation to serum dilution (y-axis) for naked MV and MV-infected BM-MSCs. Mean ± SEM. N = 6 from 3 independent experiments. (B) Representative live cell confocal images of BM-MSCs at 48 hpi with MV-NSe-GFP (MOI of 1.0), cocultured with Nalm 6 cells transduced with RFP. Images show the different stages of a fusion event between a Nalm 6 cell (red) and an infected BM-MSC (green). Scale bar represents 10 μm. (C) (i) Graph shows the percentage of Nalm 6 cells fusing (dark gray bars) or not (light gray bars) after establishing contact with infected BM-MSCs within 80 minutes of coculture (first column). Columns 2 to 4 represent the test and control conditions, with dilutions of serum or FIP, as indicated. $^{**}P < .01$; $^{*}P < .05$; NS = $P > .05$. (ii) Graph shows the increase of red fluorescence in green syncytia over 80 minutes of coculture. Columns are as for 4Ci. (D) Graph shows the contact time between Nalm 6 cells and BM-MSCs before fusion occurs, within 80 minutes of coculture. When indicated, cells were also preincubated with anti-MV antibody serum 1:128. For each of the above conditions, n > 125 cells were counted, and data are from 6 independent experiments.

immunosuppressive and myelosuppressive chemotherapy (including dexamethasone, anthracycline, vincristine, asparaginase, cyclophosphamide, and cytarabine), that clinically significant anti-MV antibodies persist in all cases, confirming the need for an alternative but clinically relevant strategy for circumvention.

We chose to investigate human BM-MSCs in our preclinical model for a number of reasons. First, MSCs are a highly clinically relevant commodity, with a wealth of data detailing the safe use of IV-delivered allogeneic or autologous BM-MSCs as a therapeutic strategy in several diseases including acute graft-versus-host disease following hematopoietic cell transplantation for hematological malignancy.[53-55] Second, MSCs are hypoimmunogenic, permitting safe administration without preconditioning. Thus, allogeneic donor-mismatched BM-MSCs can potentially be an "off the shelf" commodity, allowing their use as virotherapeutic delivery vehicles but without themselves representing a target for elimination of the therapeutic element. Third, evidence suggests that MSCs colocate and interact with ALL in the BM microenvironment.[56] Finally, based on preclinical studies investigating the migratory capacity of MSCs,[57] we hypothesized that BM-MSCs would be likely to home to BM targets on systemic infusion. One recent murine study demonstrated that systemically administered BM-MSCs can deliver oncolytic MV to localized hepatocellular carcinoma tumor targets.[58] However, the present study demonstrates for the first time the ability of BM-MSCs to enhance the efficacy of systemic measles virotherapy for a widely disseminated, BM-based malignancy such as ALL.

In addition to BM, MSCs can be isolated from a number of alternative sources, including adipose tissue.[59] Subtle differences in their in vitro immunophenotype, differentiation capacity, and gene expression profile are seen compared with BM-MSCs, but the extent to which these features lead to biological differences in vivo remains unknown, and the MSC lineage needs to be carefully and rationally considered for each particular tumor type. Although adipose-derived MSCs have been used as IP delivery vehicles for oncolytic MV in a preclinical model of ovarian cancer,[41] IV-administered BM-MSCs for the targeted delivery of an oncolytic virus to a BM-based malignancy is rapidly translatable, because it is fully compatible with current investigational and therapeutic approaches to ALL.

Our data show that in contrast to primary ALL tumor cells that typically die soon after viral infection,[22] BM-MSCs—while readily infectable by MV—retain viability at 48 hpi and continue to produce

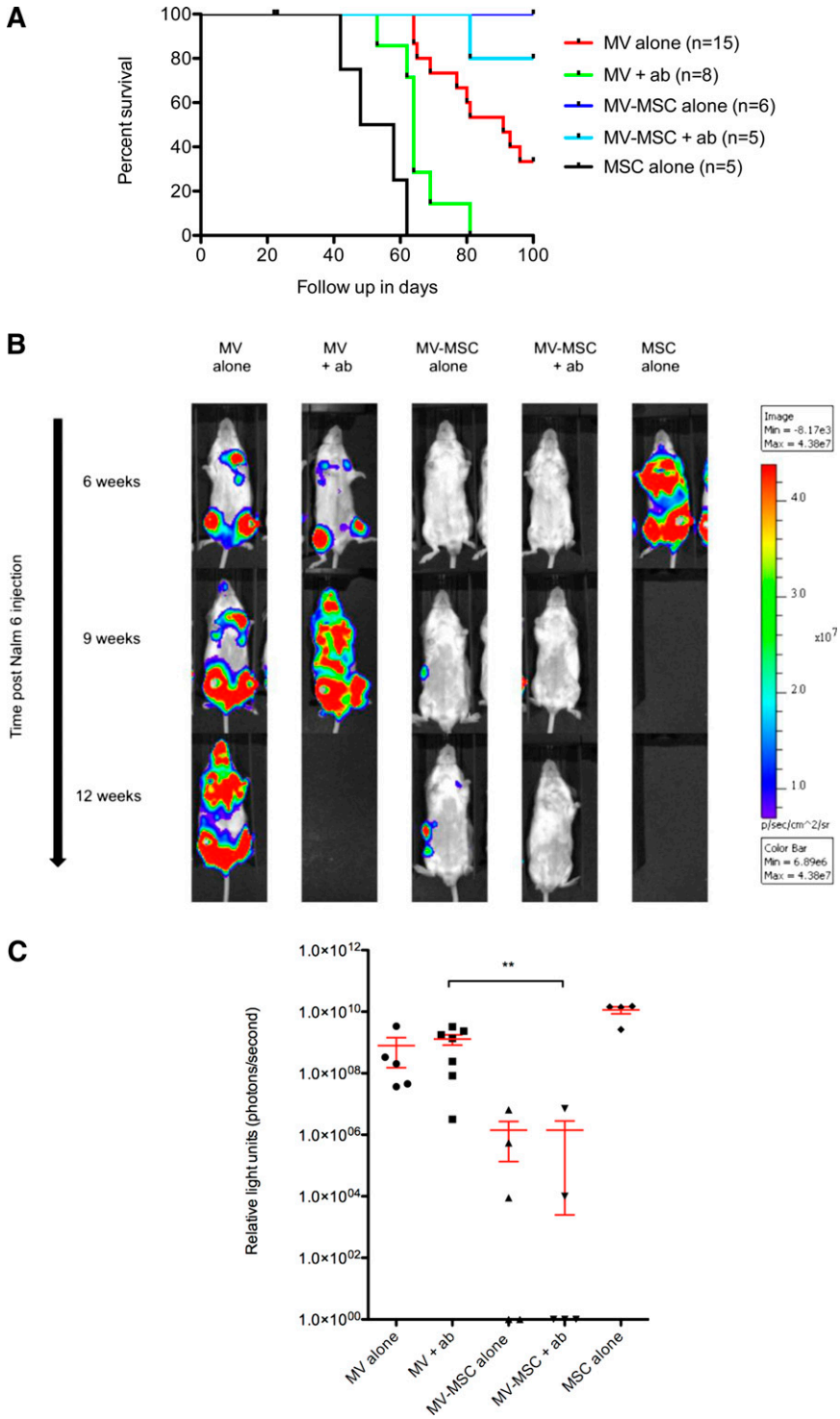

Figure 5. Therapeutic efficacy of cell carrier–delivered oncolytic measles virotherapy in a Nalm-6 disseminated model of precursor B-ALL. (A) Kaplan-Meier survival curves of mice bearing disseminated Nalm 6 xenografts treated intravenously with a total of either 1×10^6 pfu MV-NSe; 1×10^6 BM-MSCs loaded with MV-NSe at MOI of 1.0, or 1×10^6 uninfected BM-MSCs. Mice in the relevant groups also received 50 IU (100 μL) of anti-MV IgG antibody (or 100 μL PBS control) via the intraperitoneal route 3 hours before each MV injection. Data represent results from 3 independent experiments. N = 2 to 5 per group. (B) Representative bioluminescence images of SCID mice treated with naked MV, MV-infected BM-MSCs, or BM-MSCs alone in the presence or absence of anti-measles antibody–containing serum. The images demonstrate disease burden after ALL cell injection at 6, 9, and 12 weeks. Where no image is shown, this indicates that no mice remained in the relevant treatment group. (C) Scatter dot plot showing individual values for luminescent activity (photons per second) performed on each surviving animal in each treatment group at week 6. Values are represented minus background luminescent activity. Data are shown as mean ± SEM. To ensure that data for all surviving animals could be plotted, zero or negative values were arbitrarily assigned a value of 1.0. $^{**}P = .0051$.

virus. Furthermore, MV-loaded BM-MSCs localized to sites of ALL in the BM of mice following IV infusion. Before moving to therapeutic studies in mice, we were keen to precisely quantify the interaction between BM-MSCs and target ALL cells. The timescale over which virus hand-off occurs and whether this process occurs by fusion or by infection from released virus are important questions, as both parameters are likely to influence the potential success of this delivery approach in trials. Live cell confocal imaging confirmed that the majority of hand-off results from heterofusion and occurs rapidly—within 20 minutes of coculture—suggesting that virus delivery to tumor would take place in vivo long before BM-MSC viability is compromised and prior to any anamnestic response. Live cell confocal imaging was also used to visualize the impact of antiviral antibodies on this process. Heterofusion events—impossible unless MV-H and F glycoproteins are both displayed at the surface of the BM-MSCs—were predictably ablated in the presence of very high antibody concentrations and FIP, whereas at lower antibody concentrations, heterofusion events remained plentiful.

In vivo, passive immunization of animals prior to each MV administration was provided with injection of high titer anti-MV antiserum (50 IU anti-MV IgG), equating to an ultimate anti-MV antibody concentration several logs higher than the 300 mIU/mL deemed high titer in the clinical setting. This was quite sufficient to almost completely abrogate therapeutic responses to naked MV. However, successful delivery and therapeutic efficacy of BM-MSC–delivered oncolytic MV was demonstrated in this setting, suggesting successful MSC homing, virus hand-off, and ultimately therapeutic protection from repeated infusions of anti-MV antibody designed to model an anamnestic response. This is in contrast to the lack of abrogation of MV antitumor responses that we previously described when antiviral antibodies are delivered locally to MV-treated subcutaneous human B-cell lymphoma xenografts,[17] further highlighting the central importance of shielding the virus from anti-MV antibodies during systemic delivery to a disseminated malignancy. Unexpectedly, delivering MV within BM-MSC carriers also improved anti-ALL efficacy beyond that seen with naked MV. Because BM-MSCs administered alone granted no survival benefit, we hypothesize that the continuing MV replication and production within the BM-MSCs enhances the virus payload reaching distant tumor targets.

Clinical validation is now required. An initial phase 1 trial of oncolytic MV in adult ALL is planned. Alongside efforts to determine the safety of IV-administered oncolytic MV in this disease, secondary goals will include the careful monitoring of humoral and cellular responses to injected virus to set a baseline for evaluation of immune shielding approaches. The strategy proposed here is compatible with rapid translation to the clinic and does not preclude an approach alongside immunosuppressive therapy.

Acknowledgments

This work was supported by a clinical training fellowship award to A.C. from Leukaemia and Lymphoma Research UK.

Authorship

Contribution: A.C. performed the research; A.C. and A.K.F. wrote the paper; A.D. provided technical assistance with animal work; B.B. performed the MV-IgG enzyme-linked immunosorbent assay on primary patient material; B.P. edited the manuscript; A.A. and D.M.D. performed the confocal imaging and confocal data analysis, and edited the manuscript; and A.K.F. supervised the study.

Conflict-of-interest disclosure: The authors declare no competing financial interests.

Correspondence: A. K. Fielding, Department of Hematology, Royal Free Campus, University College London, Rowland Hill St, London NW3 2PF, UK; e-mail: a.fielding@ucl.ac.uk.

References

1. Larson RA, Dodge RK, Burns CP, et al. A five-drug remission induction regimen with intensive consolidation for adults with acute lymphoblastic leukemia: cancer and leukemia group B study 8811. *Blood.* 1995;85(8):2025-2037.
2. Annino L, Vegna ML, Camera A, et al; GIMEMA Group. Treatment of adult acute lymphoblastic leukemia (ALL): long-term follow-up of the GIMEMA ALL 0288 randomized study. *Blood.* 2002;99(3):863-871.
3. Hunault M, Harousseau JL, Delain M, et al; GOELAMS (Groupe Ouest-Est des Leucémies Airguës et Maladies du Sang) Group. Better outcome of adult acute lymphoblastic leukemia after early genoidentical allogeneic bone marrow transplantation (BMT) than after late high-dose therapy and autologous BMT: a GOELAMS trial. *Blood.* 2004;104(10):3028-3037.
4. Kantarjian H, Thomas D, O'Brien S, et al. Long-term follow-up results of hyperfractionated cyclophosphamide, vincristine, doxorubicin, and dexamethasone (Hyper-CVAD), a dose-intensive regimen, in adult acute lymphocytic leukemia. *Cancer.* 2004;101(12):2788-2801.
5. Takeuchi J, Kyo T, Naito K, et al. Induction therapy by frequent administration of doxorubicin with four other drugs, followed by intensive consolidation and maintenance therapy for adult acute lymphoblastic leukemia: the JALSG-ALL93 study. *Leukemia.* 2002;16(7):1259-1266.
6. Thomas X, Boiron JM, Huguet F, et al. Outcome of treatment in adults with acute lymphoblastic leukemia: analysis of the LALA-94 trial. *J Clin Oncol.* 2004;22(20):4075-4086.
7. Linker C, Damon L, Ries C, Navarro W. Intensified and shortened cyclical chemotherapy for adult acute lymphoblastic leukemia. *J Clin Oncol.* 2002; 20(10):2464-2471.
8. Gökbuget N, Hoelzer D, Arnold R, et al. Treatment of Adult ALL according to protocols of the German Multicenter Study Group for Adult ALL (GMALL). *Hematol Oncol Clin North Am.* 2000;14(6): 1307-1325..
9. Pulte D, Gondos A, Brenner H. Improvement in survival in younger patients with acute lymphoblastic leukemia from the 1980s to the early 21st century. *Blood.* 2009;113(7): 1408-1411.
10. Fielding AK, Richards SM, Chopra R, et al; Medical Research Council of the United Kingdom Adult ALL Working Party; Eastern Cooperative Oncology Group. Outcome of 609 adults after relapse of acute lymphoblastic leukemia (ALL); an MRC UKALL12/ECOG 2993 study. *Blood.* 2007; 109(3):944-950.
11. Topp MS, Gökbuget N, Zugmaier G, et al. Long-term follow-up of hematologic relapse-free survival in a phase 2 study of blinatumomab in patients with MRD in B-lineage ALL. *Blood.* 2012; 120(26):5185-5187.
12. Breitbach CJ, Reid T, Burke J, Bell JC, Kirn DH. Navigating the clinical development landscape for oncolytic viruses and other cancer therapeutics: no shortcuts on the road to approval. *Cytokine Growth Factor Rev.* 2010;21(2-3):85-89.
13. Liu TC, Galanis E, Kirn D. Clinical trial results with oncolytic virotherapy: a century of promise, a decade of progress. *Nat Clin Pract Oncol.* 2007; 4(2):101-117.
14. Park BHH, Hwang T, Liu TC, et al. Use of a targeted oncolytic poxvirus, JX-594, in patients with refractory primary or metastatic liver cancer: a phase I trial. *Lancet Oncol.* 2008;9(6):533-542.
15. Senzer NN, Kaufman HL, Amatruda T, et al. Phase II clinical trial of a granulocyte-macrophage colony-stimulating factor-encoding, second-generation oncolytic herpesvirus in patients with unresectable metastatic melanoma. *J Clin Oncol.* 2009;27(34):5763-5771.
16. Vidal L, Pandha HS, Yap TA, et al. A phase I study of intravenous oncolytic reovirus type 3 Dearing in patients with advanced cancer. *Clin Cancer Res.* 2008;14(21):7127-7137.
17. Grote D, Russell SJ, Cornu TI, Cattaneo R, Vile R, Poland GA, Fielding AK. Live attenuated measles virus induces regression of human lymphoma xenografts in immunodeficient mice. *Blood.* 2001;97(12):3746-3754.
18. Ungerechts G, Frenzke ME, Yaiw KC, Miest T, Johnston PB, Cattaneo R. Mantle cell lymphoma salvage regimen: synergy between a reprogrammed oncolytic virus and two chemotherapeutics. *Gene Ther.* 2010;17(12): 1506-1516.
19. Ungerechts G, Springfeld C, Frenzke ME, et al. Lymphoma chemovirotherapy: CD20-targeted and convertase-armed measles virus can synergize with fludarabine. *Cancer Res.* 2007; 67(22):10939-10947.
20. Dingli D, Offord C, Myers R, et al. Dynamics of multiple myeloma tumor therapy with a recombinant measles virus. *Cancer Gene Ther.* 2009;16(12):873-882.
21. Dingli D, Peng KW, Harvey ME, et al. Image-guided radiovirotherapy for multiple myeloma using a recombinant measles virus expressing the thyroidal sodium iodide symporter. *Blood.* 2004; 103(5):1641-1646.
22. Patel B, Dey A, Ghorani E, et al. Differential cytopathology and kinetics of measles oncolysis in two primary B-cell malignancies provides mechanistic insights. *Mol Ther.* 2011;19(6): 1034-1040.
23. Peng KW, TenEyck CJ, Galanis E, Kalli KR, Hartmann LC, Russell SJ. Intraperitoneal therapy of ovarian cancer using an engineered measles virus. *Cancer Res.* 2002;62(16):4656-4662.
24. Peng KW, Hadac EM, Anderson BD, et al. Pharmacokinetics of oncolytic measles virotherapy: eventual equilibrium between virus and tumor in an ovarian cancer xenograft model. *Cancer Gene Ther.* 2006;13(8):732-738.

25. Allen C, Paraskevakou G, Liu C, et al. Oncolytic measles virus strains in the treatment of gliomas. *Expert Opin Biol Ther.* 2008;8(2):213-220.
26. Allen C, Vongpunsawad S, Nakamura T, et al. Retargeted oncolytic measles strains entering via the EGFRvIII receptor maintain significant antitumor activity against gliomas with increased tumor specificity. *Cancer Res.* 2006;66(24): 11840-11850.
27. Studebaker AW, Kreofsky CR, Pierson CR, Russell SJ, Galanis E, Raffel C. Treatment of medulloblastoma with a modified measles virus. *Neuro-oncol.* 2010;12(10):1034-1042.
28. McDonald CJ, Erlichman C, Ingle JN, et al. A measles virus vaccine strain derivative as a novel oncolytic agent against breast cancer. *Breast Cancer Res Treat.* 2006;99(2):177-184.
29. Iankov ID, Msaouel P, Allen C, et al. Demonstration of anti-tumor activity of oncolytic measles virus strains in a malignant pleural effusion breast cancer model. *Breast Cancer Res Treat.* 2010;122(3):745-754.
30. Peng KW, Ahmann GJ, Pham L, Greipp PR, Cattaneo R, Russell SJ. Systemic therapy of myeloma xenografts by an attenuated measles virus. *Blood.* 2001;98(7):2002-2007.
31. Heinzerling L, Künzi V, Oberholzer PA, Kündig T, Naim H, Dummer R. Oncolytic measles virus in cutaneous T-cell lymphomas mounts antitumor immune responses in vivo and targets interferon-resistant tumor cells. *Blood.* 2005;106(7): 2287-2294.
32. Galanis E, Hartmann LC, Cliby WA, et al. Phase I trial of intraperitoneal administration of an oncolytic measles virus strain engineered to express carcinoembryonic antigen for recurrent ovarian cancer. *Cancer Res.* 2010;70(3):875-882.
33. Schneider U, Bullough F, Vongpunsawad S, Russell SJ, Cattaneo R. Recombinant measles viruses efficiently entering cells through targeted receptors. *J Virol.* 2000;74(21):9928-9936.
34. Hammond AL, Plemper RK, Zhang J, Schneider U, Russell SJ, Cattaneo R. Single-chain antibody displayed on a recombinant measles virus confers entry through the tumor-associated carcinoembryonic antigen. *J Virol.* 2001;75(5): 2087-2096.
35. Bucheit AD, Kumar S, Grote DM, et al. An oncolytic measles virus engineered to enter cells through the CD20 antigen. *Mol Ther.* 2003;7(1): 62-72.
36. Peng KW, Donovan KA, Schneider U, Cattaneo R, Lust JA, Russell SJ. Oncolytic measles viruses displaying a single-chain antibody against CD38, a myeloma cell marker. *Blood.* 2003;101(7): 2557-2562.
37. Peng KW, Holler PD, Orr BA, Kranz DM, Russell SJ. Targeting virus entry and membrane fusion through specific peptide/MHC complexes using a high-affinity T-cell receptor. *Gene Ther.* 2004; 11(15):1234-1239.
38. Peng KW, Facteau S, Wegman T, O'Kane D, Russell SJ. Non-invasive in vivo monitoring of trackable viruses expressing soluble marker peptides. *Nat Med.* 2002;8(5):527-531.
39. Myers RM, Greiner SM, Harvey ME, et al. Preclinical pharmacology and toxicology of intravenous MV-NIS, an oncolytic measles virus administered with or without cyclophosphamide. *Clin Pharmacol Ther.* 2007;82(6):700-710.
40. Liu C, Russell SJ, Peng KW. Systemic therapy of disseminated myeloma in passively immunized mice using measles virus-infected cell carriers. *Mol Ther.* 2010;18(6):1155-1164.
41. Mader EK, Maeyama Y, Lin Y, et al. Mesenchymal stem cell carriers protect oncolytic measles viruses from antibody neutralization in an orthotopic ovarian cancer therapy model. *Clin Cancer Res.* 2009;15(23):7246-7255.
42. Ong HT, Hasegawa K, Dietz AB, Russell SJ, Peng KW. Evaluation of T cells as carriers for systemic measles virotherapy in the presence of antiviral antibodies. *Gene Ther.* 2007;14(4): 324-333.
43. Iankov ID, Blechacz B, Liu C, et al. Infected cell carriers: a new strategy for systemic delivery of oncolytic measles viruses in cancer virotherapy. *Mol Ther.* 2007;15(1):114-122.
44. Ilett EJ, Prestwich RJ, Kottke T, et al. Dendritic cells and T cells deliver oncolytic reovirus for tumour killing despite pre-existing anti-viral immunity. *Gene Ther.* 2009;16(5):689-699.
45. Munguia A, Ota T, Miest T, Russell SJ. Cell carriers to deliver oncolytic viruses to sites of myeloma tumor growth. *Gene Ther.* 2008;15(10): 797-806.
46. Ahmed AU, Tyler MA, Thaci B, et al. A comparative study of neural and mesenchymal stem cell-based carriers for oncolytic adenovirus in a model of malignant glioma. *Mol Pharm.* 2011; 8(5):1559-1572.
47. Thaci B, Ahmed AU, Ulasov IV, et al. Pharmacokinetic study of neural stem cell-based cell carrier for oncolytic virotherapy: targeted delivery of the therapeutic payload in an orthotopic brain tumor model. *Cancer Gene Ther.* 2012;19(6):431-442.
48. Wei J, Wahl J, Nakamura T, et al. Targeted release of oncolytic measles virus by blood outgrowth endothelial cells in situ inhibits orthotopic gliomas. *Gene Ther.* 2007;14(22): 1573-1586.
49. Horwitz EM, Le Blanc K, Dominici M, et al; International Society for Cellular Therapy. Clarification of the nomenclature for MSC: The International Society for Cellular Therapy position statement. *Cytotherapy.* 2005;7(5):393-395.
50. Karber G. 50% End point calculation *Arch Exp Pathol Pharmakol.* 1931(162); 162:480-483.
51. Pfaffl MW. A new mathematical model for relative quantification in real-time RT-PCR. *Nucleic Acids Res.* 2001;29(9):e45.
52. Peng KW, Myers R, Greenslade A, et al. Using clinically approved cyclophosphamide regimens to control the humoral immune response to oncolytic viruses. *Gene Ther.* 2013;20(3): 255-261.
53. Le Blanc K, Frassoni F, Ball L, et al; Developmental Committee of the European Group for Blood and Marrow Transplantation. Mesenchymal stem cells for treatment of steroid-resistant, severe, acute graft-versus-host disease: a phase II study. *Lancet.* 2008;371(9624): 1579-1586.
54. Ringdén O, Uzunel M, Rasmusson I, et al. Mesenchymal stem cells for treatment of therapy-resistant graft-versus-host disease. *Transplantation.* 2006;81(10):1390-1397.
55. Kebriaei P, Isola L, Bahceci E, et al. Adult human mesenchymal stem cells added to corticosteroid therapy for the treatment of acute graft-versus-host disease. *Biol Blood Marrow Transplant.* 2009;15(7):804-811.
56. Iwamoto S, Mihara K, Downing JR, Pui CH, Campana D. Mesenchymal cells regulate the response of acute lymphoblastic leukemia cells to asparaginase. *J Clin Invest.* 2007;117(4): 1049-1057.
57. Dittmar T, Entschladen F. Migratory Properties of Mesenchymal Stem Cells. Berlin, Germany: Springer; 2012.
58. Ong HT, Federspiel MJ, Guo CM, et al. Systemically delivered measles virus-infected mesenchymal stem cells can evade host immunity to inhibit liver cancer growth. *J Hepatol.* 2013; 59(5):999-1006.
59. Zuk PA, Zhu M, Mizuno H, et al. Multilineage cells from human adipose tissue: implications for cell-based therapies. *Tissue Eng.* 2001;7(2):211-228.